

Efficient line tracker in the parameter space based on one-to-one Hough Transform

Yannick Wend Kuni Zoetgnande¹ and Antoine Manzanera²

¹Laboratoire Traitement du Signal et de l'Image, INSERM U1099, Université de Rennes 1, FRANCE

²U2IS-Autonomous Systems and Robotics, ENSTA ParisTech, Université de Paris Saclay, FRANCE
antoine.manzanera@ensta-paristech.fr; yannick.zoetgnande@etudiant.univ-rennes1.fr

Keywords: Video Analysis, Line Tracking, Real-Time, Hough Transform.

Abstract: We propose a new method for line detection and tracking in videos in real-time. It is based on an optimised version of the dense Hough transform, that computes, via one-to-one projection, an accumulator in the polar parameter space using the gradient direction in the grayscale image. Our method then performs mode (cluster) tracking in the Hough space, using prediction and matching of the clusters based on both their position and appearance. The implementation takes advantage of the high performance video processing library Video++, that allows to parallelise simply and efficiently many video primitives.

1 Introduction

Feature tracking in videos, which consists in detecting particular points or subsets in each image and match them with their counterparts in the following images of the sequence, is a fundamental problem of computer vision. Unlike feature points or object tracking, for which the literature is plethora, line tracking has not received so much attention (Wang et al., 2009). However, in both mathematical and combinatorial terms, the (1d) line represents a relevant trade-off between the (0d) point and the (2d) region (or plane, or facet). Furthermore detecting and matching lines along a video sequence has many useful applications, in mobile robotics (Fontanelli et al., 2015), visual servoing, image registration (Fung and Wong, 2013b) or 3d reconstruction (Kim and Manduchi, 2017).

In this paper we present a fast line tracking algorithm designed to detect and match lines along video sequences in real-time. The proposed method leverages three complementary frameworks:

- a fast line detection is performed by using the one-to-one Hough Transform
- an efficient implementation is made possible by using the *Video++* high performance video processing library
- a tracking algorithm is applied in the Hough \times time space, combining prediction and fast mode

matching

The paper is structured as follows: Section 2 summarizes the related work, first in Hough based line detection and then in tracking in the Hough space. Section 3 details the different parts of our algorithm and implementation framework. Section 4 presents some results, including computational performances. Finally Section 5 concludes the paper and presents some perspectives.

2 Related works

2.1 Hough based line detection

Since its introduction in the early 60's for detecting line beams in bubble chamber's images (Hough, 1962), the Hough transform (HT) has been the subject of many studies, with thousands of citations and references.

The general framework consists in detecting parameterised shapes in images using accumulators in parameter spaces. More formally, if a shape is defined by a parametric equation $f(\mathbf{x}, \pi) = 0$, with $\mathbf{x} \in I$ a point in the image space, and $\pi \in \mathcal{P}$ a point in the parameter space, the shape in the image space is defined as:

$$C_{\pi}^I = \{\mathbf{x} \in I; f(\mathbf{x}, \pi) = 0\}$$

whereas the dual shape in the parameter space is defined as:

$$C_x^p = \{\pi \in \mathcal{P}; f(\mathbf{x}, \pi) = 0\}$$

Now consider a set of points from the image space: $\mathcal{S} \subset I$, the Hough Transform of \mathcal{S} can be formally defined as:

$$HT(\mathcal{S}) = \bigcup_{\mathbf{x} \in \mathcal{S}} C_x^p$$

For line detection, polar parameterisation is used (Duda and Hart, 1972). It represents a line by the angle θ made by its normal with the abscissa axis, and its distance ρ to the origin. Then the image variable $\mathbf{x} = (x, y)$ and the parameter variable $\pi = (\theta, \rho)$, are linked by the equation:

$$\rho = x \cos \theta + y \sin \theta \quad (1)$$

Using this parametrisation, the dual shape of line is a sinusoid. The main drawback of traditional Hough Transforms is their computational cost. This explains why, even restricting to line detection, many variants and optimisations of the basic framework have been proposed (Herout et al., 2013). We shall group them into three categories:

- **One-to-many / Probabilistic HT** The image space is reduced to a small number of representative (contour) points. Then, every point of the image space will vote for many points representing a sinusoid in the parameter space. In this case, the number of voting (contour) points, and also the quantization of the parameter space are critical for the complexity. In the probabilistic version (Kiryati et al., 1991), the complexity is decreased by reducing the number of voting points to a small portion of contour pixels.
- **Many-to-one / Randomised HT** The image space is also reduced to contour points, but here, every pair of contour points, defining a unique line, votes for a single point in the parameter space. To reduce the high combinatorics, the randomised version (Xu et al., 1990), only draws randomly a small number of pairs of contour pixels. One advantage with respect to the previous approach is that the parameter space does not need to be quantized as a 2d array, making the line selection more flexible.
- **One-to-one / Dense HT** It was early noticed that the knowledge of the gradient orientation was sufficient to get the equation of a line possibly passing at any point (O’Gorman and Clowes, 1976). This allows to directly estimate the parameters

at any location (dense estimation) without computing the contours, and using one-to-one voting. (Manzanera et al., 2016) proposed a unified one-to-one dense HT for lines and circles, based on multiscale derivatives. Like the previous approaches, quantization of the parameter space is no longer necessary, and the clustering can be made on-the-fly, which is particularly interesting in the case of line tracking. The 1-to-1 DHT is detailed on Algorithm 1.

Algorithm 1 Dense 1-to-1 Hough Transform

Require: Image I ▷ The Image
1: **for each** $pixel(p_x, p_y) \in \{0, w_I\} \times \{0, h_I\}$ **do** ▷
 w_I, h_I resp. width, height
2: $\nabla I \leftarrow (I_x(p), I_y(p))$
3: **if** $\|\nabla I\| > 0$ **then**
4: $d \leftarrow p_x I_x + p_y I_y$
5: $\rho \leftarrow \frac{|d|}{\|\nabla I\|}$
6: $\theta = \arctan(\frac{I_y}{I_x})$
7: $\Gamma(\rho, \theta) \leftarrow \Gamma(\rho, \theta) + \|\nabla I\|$ ▷ Γ is the accumulator

2.2 Tracking in the Hough space

A significant amount of works on line tracking have been using Hough Transform, but for most of them, the tracking is actually performed in the image space, the HT being just used to detect dominant lines. (Marchant, 1996) uses HT to follow crop rows in automated agriculture. (Voisin et al., 2005) and (Borkar et al., 2009) also use HT to detect road marks, and track them in the image space. (Foresti, 1998) uses line matching to track multiple objects. (Behrens et al., 2001) combine a Randomized HT and a discrete Kalman filter to track tubular features in medical images.

(Hills et al., 2003) propose a method to track objects in the Hough space. Their objective is to follow objects that can be circumscribed by parallel lines, like rectangular objects. Another limitation is that the tracking is only performed frame to frame, without memory. To deal with these limits (Mills et al., 2003) use an extended Kalman filter, to address the non linearity due to the polar parameter space. In the Hough space the line number i at the k th frame is identified by (ρ_i^k, θ_i^k) . At the $(k+1)$ th frame the position of the line will be assumed to vary smoothly, to reduce the computational load of the HT. Unfortunately in real world situation, edges are not always parallel and it is very hard to determine the best setting of each Kalman filter. So this model performs well when the number of

edges is small or when their motion is simple enough.

To overcome these drawbacks, (Fung and Wong, 2013b) propose a robust tracking method based on a multiple Kalman filter. Instead of associating each edge to one Kalman filter, they use N concurrent sub-Kalman filters, and the best prediction is returned at the end. The Kalman filters are run in parallel and their updates are performed at the same time. The final prediction is the weighted sum of the predictions from all filters. Later, (Fung and Wong, 2013a) they propose another method to detect and track quadrangles.

However these two last methods do not track more than four lines. Furthermore, if they are able to deal with line occlusion, they do not take into account entries and exits. In addition, they are all based on classic contour-based HTs.

3 Our method

3.1 Preliminaries

Let $P = (\theta_P, \rho_P)$ and $Q = (\theta_Q, \rho_Q)$ be two points in the parameter (Hough) space. Let $\Gamma(P)$ be the value of the HT (accumulator) at point P .

The distance between P and Q in the parameter space is defined as:

$$d_{\mathcal{P}}(P, Q) = \sqrt{D_I^2 \sin^2(\theta_P - \theta_Q) + (\rho_P - \rho_Q)^2} \quad (2)$$

where D_I is the diagonal size of the image. This definition takes into account the modularity of angle difference, and also the fact that, when ρ is close to 0, the lines defined by parameters (θ, ρ) and $(\pi - \theta, \rho)$ are very close in the image space.

We also use the similarity metrics in the Hough accumulator, defined as follows:

$$d_{\Gamma}(P, Q)^2 = \sum_{d_{\theta}=-\Delta_{\theta}}^{+\Delta_{\theta}} \sum_{d_{\rho}=-\Delta_{\rho}}^{+\Delta_{\rho}} [\Gamma(\theta_P + d_{\theta}, \rho_P + d_{\rho}) - \Gamma(\theta_Q + d_{\theta}, \rho_Q + d_{\rho})]^2 \quad (3)$$

3.2 Video++ library

Video++ (Garrigues and Manzanera, 2014) is a library written in C++14 whose purpose is to allow the fast development of high performance video processing applications. It manages memory allocation and alignment, pixel accesses and simple writing of pixel-wise and neighborhood operations. By using meta-

programming based on lambda functions and variadic templates, it generates code that is both concise and easy to optimize and parallelize using *G++6* and *OpenMP*.

It has been shown (Garrigues and Manzanera, 2014) that Video++ was more efficient than *OpenCV* on local and regular operations, and as fast as the raw *OpenMP* version, while being much more concise. The dense 1-to-1 HT being essentially regular, and the tracking functions highly parallelisable, Video++ seems a good framework for implementing our algorithm.

3.3 Dense one-to-one Hough Transform

3.3.1 Voting process

We implemented the 1-to-1 dense voting process (Algorithm 1) on Video++, enabling parallelisation of the gradient and parameter computation (lines 2-6) and of the voting process (line 7). The problem of concurrent access to Γ happens overall when the clustering is performed with K-means or Hierarchical clustering. In 1-to-1 DHT, like in many-to-one HT, the vote is casted for one single point, which makes the resulting voting map sparse. To moderate it, the parameters are estimated in float precision for every pixel, and the votes are interpolated and divided between the 4 closest quantized values.

3.3.2 Selection of the N dominant lines

In order to avoid multiple detections, we use a non-maxima suppression through a copy of the Hough space noted Γ' , by putting $\Gamma'(P) = 0$ to every cell P such that there exist another cell Q in the $\lambda_{\theta} \times \lambda_{\rho}$ neighborhood of P such that $\Gamma(Q) > \Gamma(P)$. This process is fully parallelized using SIMD paradigm because the search is performed in Γ and the updates are performed in Γ' . To reduce the computational cost, we only apply non-maxima suppression to cells where Γ exceeds a certain threshold.

Finally the N dominant lines are extracted as the N greatest values of Γ' , sorted in descendant order: $C = \{C_1, \dots, C_N\}$, and such that the values of C_i are obtained in float precision as the weighted average of the 9 neighbors that surround the maximum in the quantized parameter space. The weighting corresponds to the number of votes obtained by each cell. In our experiments, the default value of N is 50 and the couple $(\lambda_{\theta}, \lambda_{\rho})$ is initialized to (15, 12). During the tracking this value can change depending on the density of clusters.

3.4 Tracking in the Hough space

Our tracking procedure is based on several common assumptions, as used by previously mentioned works (Mills et al., 2003; Yilmaz et al., 2006; Fung and Wong, 2013b):

- *Proximity*: the position of a feature does not change much between two frames.
- *Maximum velocity*: the apparent velocity of a feature in the image is upper bounded.
- *Small velocity change*: the acceleration of the feature is small.
- *Common motion*: neighboring features have similar velocity.

We also use the two following specific assumptions:

- *Smooth changes in the contrast order*: if a line is ranked in j th position at frame t , it should be ranked between positions $j - \alpha$ and $j + \alpha$ th at frame $t + 1$.
- *Smooth changes of the line beams*: Between two possible closest matches, the best is the one whose neighborhood is the closest in the Hough space.

The Algorithm 2 details the complete tracking procedure. It starts from a list of M so-called *clusters*, corresponding to the current tracked lines represented by their parameters, their life time (the number of frames they have existed) and their inactivity time (the number of frames since when they have not been updated).

The matching between clusters and the new lines is made using the N best dominant lines, with $N > M$, since a line can be less dominant from one frame to the other. We take into account line occlusions, exits and entries. First when a cluster becomes more dominant it enters the list of most dominant clusters. Second when a cluster become less dominant it exits the same list. And third when two clusters at frame t match the same line at frame $t + 1$, it means that one of clusters occludes the other one. The most dominant is kept in that case.

So each cluster at frame t is compared to 2α lines at frame $t + 1$. The first match is performed by considering only the position of clusters in the parameter space, providing at most three best matches for each cluster whose distance is less than some threshold. Then the neighborhood of the cluster in the accumulator array is compared to the neighborhood of each of the three candidates and the best matches is

retained. The new best clusters are then added to the list of the current clusters.

In the algorithm 2 we have:

- The set $\mathcal{C} = \{P_1^t, P_2^t, \dots, P_M^t\}$ represents the list of dominant lines (clusters) at time t . The number M is not fixed and is linked to the number of clusters whose value in Γ is greater than a certain threshold noted $\Gamma_{threshold}$, but it has to remain significantly less than N .
- To each cluster P_i^t we associate the value fwu representing the number of consecutive frames where it got no update.
- The set $\Upsilon = \{Q_1, Q_2, \dots, Q_N\}$ represents the list of N dominant lines detected. Their value have not to be greater than $\Gamma_{threshold}$, and their number N must be greater than $M + \alpha$.
- To each cluster P_i^t we associate at most three best matches according to their proximity in the Hough space. We will denote those three best matches by Ψ_i (lines 7-11).
- mt_i^t represents a motion threshold for the cluster P_i^t . It prevents the cluster to be associated if its nearest neighbor is too far. It can be chosen as a constant, or depend on the cluster i and the frame t , to adapt to the dynamics of the different lines.
- Finally, the clusters that have not been associated for more than $mfwu$ successive frames are removed from the cluster list (exits, lines 17-19), and the new lines, i.e. those that have not been associated to an existing cluster, and that are more dominant than some cluster, are added to the cluster list (entries, lines 20-22).

4 Results

4.1 Dense one-to-one Hough Transform

We evaluate in this section the computation time of the 1-to-1 dense HT implemented with Video++ on a 8-core computer with Intel Core i7, 2.40 GHz, and compare it with the Standard Hough Transform (SHT) and an optimized version of the Progressive Probabilistic Hough Transform (PPHT) of OpenCV (Matas et al., 2000). So we use three images (Fig.1 to 3) and for each type of HT, we launch the algorithm 1000 times to get an accurate comparison. For the array accumulator Γ , we use a 256 values for θ , and the resolution of the image determines the number of

Algorithm 2 Line_Tracking_Hough_Space

```
1: for each frame  $t$  do
2:    $\Gamma \leftarrow \text{Dense\_Hough\_Transform}(I_t)$ 
3:    $\Upsilon \leftarrow \text{Select\_Best\_Lines}(\Gamma, N)$ 
4:   if  $t = 0$  then
5:      $\mathcal{P}^0 = \{P_1^0, \dots, P_M^0\}$ 
6:   else
7:     for each  $P_i^{t-1} \in \mathcal{P}^{t-1}$  do
8:       for each  $Q_j \in \Upsilon$  do
9:         if  $(i - \alpha \leq j \leq i + \alpha)$  then
10:          if  $d_p(P_i^{t-1}, Q_j) \leq mt_i$  then
11:            update  $\Psi^t = \{\Psi_1^t, \Psi_2^t, \Psi_3^t\}$ 
12:          for each  $P_i^{t-1} \in \mathcal{P}^{t-1}$  do
13:            if  $\Psi^t = \emptyset$  then
14:               $P_i.fwu++$ 
15:            else
16:               $P_i^t = \arg \min_{Q_k \in \Psi^t} d_\Gamma(P_i^{t-1}, Q_k)$ 
17:          for each  $P_i^t \in \mathcal{P}^t$  do
18:            if  $P_i.fwu \geq mfwu$  then
19:              Delete  $P_i^t$  from  $\mathcal{P}^t$ 
20:          for each  $Q_j \in \Upsilon$  do
21:            if  $Q_j \notin \mathcal{P}^t$  and  $\Gamma(Q_j) > \Gamma(P_M^t)$  then
22:              add  $Q_j$  to  $\mathcal{P}^t$ 
```

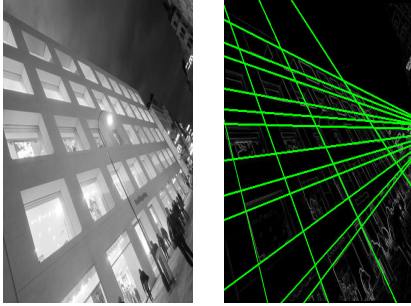


Figure 1: Building 563 × 422

values for ρ . To get a very fast and accurate computation of the arctangent, we used the approximation proposed in (Rajan et al., 2006). This approximation presents the advantage to consume less memory than a lookup table and is three times faster than the implementation of arctangent in GCC.

As shown in the table 1, our DHT algorithm (row 3) performs better than the implementations of SHT (row 1) and PPHT (row 2) in OpenCV. If needed, it can be made even faster by adding a threshold parameter th on Algorithm 1, by computing the HT only if the magnitude of the gradient is greater than th . This then corresponds to the *Semi-Dense* HT.

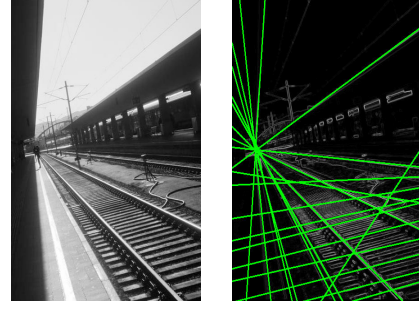


Figure 2: Subway 422 × 563

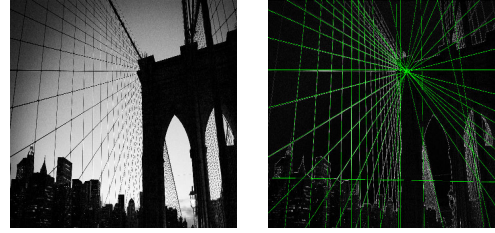


Figure 3: Bridge 2560 × 1600

	building	subway	bridge
SHT (th = 100)	20	60	2206
PPHT (th = 100)	13	17	155
DHT (th = 0)	6.2	6	69
DHT (th = 100)	3.1	3.2	32

Table 1: Comparison of computation time (in ms) with other HT methods

We have separately assessed the execution time of each part of the Dense one-to-one Hough Transform: (1) computation of the gradient of the whole image, (2) the HT itself, i.e. computing the parameters and voting (3) the search of the dominant lines. To get relevant results we launched the program 1000 times on each of the three images. For the true Dense HT, i.e. without using a threshold for the gradient, the results can be seen in Table 2. For the Semi-Dense HT ($th = 100$), results are displayed on Table 3.

	subway	building	bridge
Gradient	0.3	0.3	8
Hough Transform	2.8	2.6	51
Dominant lines	3	3.2	10

Table 2: Computation time (in ms) for each part of the DHT

4.2 Tracking in the Hough space

For optimization purposes we compute the DHT in the whole image only every r frame, the rest of the time, it can be computed only in the neighborhood

	subway	building	bridge
Gradient	0.3	0.3	8
Hough Transform	0.3	0.3	16
Dominant lines	2.5	2.6	8

Table 3: Computation time (in ms) for each part of the Semi-Dense Hough transform ($th = 100$)

	Normal	Optimized
Moving paper 1	10 ms	8 ms
Corridor 1	12 ms	10 ms
Corridor 2	12 ms	11 ms

Table 4: Computation time for tracking, per frame

of existing clusters or by defining a gradient threshold. The parameter r is set to 5 in our experiments. We intend to adapt the value of r depending on the quality of the tracking. This allows to decrease significantly the computational time because this semi-dense Hough transform is sparser.

Sometimes there are not many entries (new lines) or the existing lines (clusters) do not move fast, so we can constrain each cluster into a box ($\rho \mp \tau \times d\rho, \theta \mp \tau \times d\theta$). We have assessed each part of our tracking algorithm. The objective is to show the effectiveness of our optimizations. We use three videos that can be downloaded from (Zoetgnande, 2017).

As shown in Table 4, we have a gain in computation time, due to the fact the DHT is not computed in the whole image. Sometimes the gain is not significant because, for every pixel, we must check if it belongs to the neighborhood of a already detected line.

To each cluster we associate a random color to visually differentiate it from the others. In Fig. 4 and 5, we track clusters in the Hough space and back-project the result in the image space.

In Fig. 5, we track lines in a corridor and each line is characterized by a beam of points. More a line is spread in the image, more this line is moving. As the color is generated randomly, some lines may visually look the same.

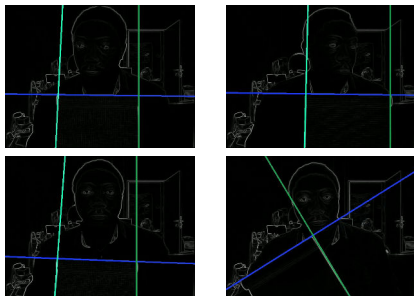


Figure 4: Result of tracking on "Moving paper" with a frame size 640×480

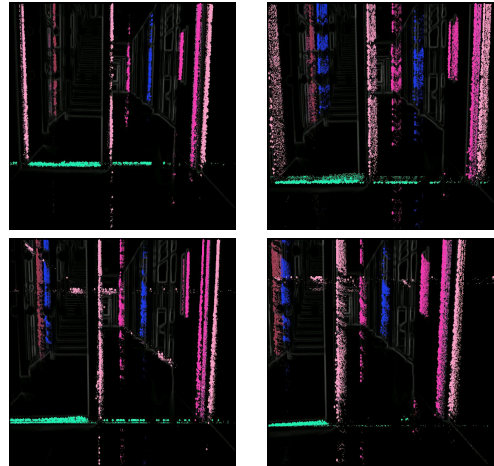


Figure 5: Result of tracking on "Corridor 1" with a frame size 640×480

5 Conclusion

In a human-made environment, there are a lot of lines. We have implemented a dense one-to-one Hough transform that can densely detect a large amount on lines on real images. Our implementation uses the library Video++ so we can get better computational performance compared to applications in OpenCV library. In 640×400 videos, we can compute the Hough transform in around 6 ms, which represents more than 150 frames per second.

Our second significant contribution concerns the tracking in the Hough space. The tracking is not only performed in the neighborhood in terms of cluster coordinates but also in terms of ranking in the list of dominant lines. Depending on the time requirements, the application can automatically adjust the number of lines to track, as well as the computation frequency of the new lines, and the size of the neighborhoods in the matching procedure.

The DHT has the advantage to output a Hough accumulator that can be used for not only point tracking but also appearance tracking. We have proposed several optimizations that improve the frame rate without affecting too much the quality of the tracker. We have tested our tracker in three videos, and showed that the whole process was computed in around 10 ms per frame.

Using the assumption that the order in the accumulator values of dominant lines should not change dramatically from one frame to the other, we can improve both the robustness and the efficiency of our tracker. One limitation of line trackers being their

poor interest in natural environment, it would be interesting to couple it with efficient point trackers (Garrigues et al., 2014), to be able to track different kind of objects depending on the context and on image content.

Acknowledgment

The authors wish to warmly thank Matthieu Garrigues for his help in the Video++ framework.

REFERENCES

- Behrens, T., Rohr, K., and Stiehl, H. S. (2001). Using an extended Hough transform combined with a Kalman filter to segment tubular structures in 3d medical images. In *Structures in 3D Medical Images. Workshop Vision, Modeling, and Visualization*, pages 491–498.
- Borkar, A., Hayes, M., and Smith, M. T. (2009). Robust lane detection and tracking with RANSAC and Kalman filter. In *16th IEEE International Conference on Image Processing*, pages 3261–3264. IEEE.
- Duda, R. O. and Hart, P. E. (1972). Use of the Hough transformation to detect lines and curves in pictures. *Communications of the ACM*, 15(1):11–15.
- Fontanelli, D., Macii, D., and Rizano, T. (2015). A fast and lowcost visionbased line tracking measurement system for robotic vehicles. *Acta IMEKO*, 4(2).
- Foresti, G. L. (1998). A line segment based approach for 3d motion estimation and tracking of multiple objects. *International journal of pattern recognition and artificial intelligence*, 12(06):881–900.
- Fung, H. K. and Wong, K. H. (2013a). Quadrangle detection based on a robust line tracker using multiple Kalman models. *Journal of ICT Research and Applications*, 7(2):137–150.
- Fung, H. K. and Wong, K. H. (2013b). A robust line tracking method based on a multiple model Kalman filter model for mobile projector systems. *Procedia Technology*, 11:996–1002.
- Garrigues, M. and Manzanera, A. (2014). Video++, a modern image and video processing C++ framework. In *Design and Architectures for Signal and Image Processing (DASIP), 2014 Conference on*, pages 1–6. IEEE.
- Garrigues, M., Manzanera, A., and Bernard, T. M. (2014). Video extruder: a semi-dense point tracker for extracting beams of trajectories in real time. *Journal of Real-Time Image Processing*, pages 1–14.
- Herout, A., Dubska, M., and Havel, J. (2013). Review of Hough transform for line detection. In *Real-Time Detection of Lines and Grids*, pages 3–16. Springer.
- Hills, M., Pridmore, T., and Mills, S. (2003). Object tracking through a Hough space. In *International Conference on Visual Information Engineering*, pages 53–56.
- Hough, P. V. (1962). Method and means for recognizing complex patterns. US Patent 3,069,654.
- Kim, C. and Manduchi, R. (2017). Indoor manhattan spatial layout recovery from monocular videos via line matching. *Computer Vision and Image Understanding*, 157:223 – 239.
- Kiryati, N., Eldar, Y., and Bruckstein, A. M. (1991). A probabilistic Hough transform. *Pattern Recognition*, 24(4):303–316.
- Manzanera, A., Nguyen, T. P., and Xu, X. (2016). Line and circle detection using dense one-to-one Hough transforms on greyscale images. *EURASIP Journal on Image and Video Processing*, 2016(1):46.
- Marchant, J. (1996). Tracking of row structure in three crops using image analysis. *Computers and electronics in agriculture*, 15(2):161–179.
- Matas, J., Galambos, C., and Kittler, J. (2000). Robust detection of lines using the progressive probabilistic Hough transform. *Computer Vision and Image Understanding*, 78(1):119 – 137.
- Mills, S., Pridmore, T. P., and Hills, M. (2003). Tracking in a Hough space with the extended Kalman filter. In *British Machine Vision Conference*, pages 1–10.
- O’Gorman, F. and Clowes, M. (1976). Finding picture edges through collinearity of feature points. *IEEE Transaction on Computers*, 25(4):449–456.
- Rajan, S., Wang, S., Inkol, R., and Joyal, A. (2006). Efficient approximations for the arctangent function. *IEEE Signal Processing Magazine*, 23(3):108–111.
- Voisin, V., Avila, M., Emile, B., Begot, S., and Bardet, J.-C. (2005). Road markings detection and tracking using Hough transform and Kalman filter. In *Advanced Concepts for Intelligent Vision Systems*, pages 76–83. Springer.
- Wang, Z., Wu, F., and Hu, Z. (2009). MSLD: A robust descriptor for line matching. *Pattern Recognition*, 42(5):941 – 953.
- Xu, L., Oja, E., and Kultanen, P. (1990). A new curve detection method: randomized Hough transform (RHT). *Pattern recognition letters*, 11(5):331–338.
- Yilmaz, A., Javed, O., and Shah, M. (2006). Object tracking: A survey. *Acm computing surveys (CSUR)*, 38(4):13.
- Zoetgnande, Y. (2017). Videos of lines to track. https://www.dropbox.com/sh/4x0aamffxx5c448/AACHN6K0o6IvvIs-_PE7apAWa?dl=0. Accessed: 2017-09-11.